Appl. Sci. Converg. Technol. 26(1): 1-5 (2017)
http://dx.doi.org/10.5757/ASCT.2017.26.1.1

Research Paper

Effect of The Impeller Discharge Angle on the Performance of a Spurt Vacuum Pump

Ji-Gu Lee[a] and Youn-Jea Kim[b]*
[a]*Graduated School of Mechanical Engineering, Sungkyunkwan University, Suwon 16419, Republic of Korea*
[b]*School of Mechanical Engineering, Sungkyunkwan University, Suwon 16419, Republic of Korea*

Received November 8, 2016; revised November 29, 2016; accepted December 1, 2017

Abstract The spurt vacuum pump is widely used to transfer sludge and slurry, and to control flow rate in a variety of processing fields, such as the oil, chemical, and fiber industries. The efficiency of the pump depends on the design parameters of the impeller, such as the number of blades, and the blade angle. In this study, the effect of the configuration of the impeller discharge angle of a spurt vacuum pump, which influences total head, shaft power, and efficiency, was numerically investigated using the commercial code, ANSYS CFX ver. 16.1. In addition, the performance of the pump was evaluated on the basis of the correlations between the total head, pump efficiency, and pressure distribution.

Keywords: Sludge and slurry, Total head, Spurt vacuum pump

I. Introduction

The spurt vacuum pump can transfer working fluid through suction and discharge processes by the rotation of a specially designed impeller. It has been widely utilized for various functions to transfer wastewater, sewage, chemical sludge and slurry. As the industry advances, the throughput of different types of wastewater according to production has continued to increase. In addition, with the environment being positioned as one of the key elements of the industry, demand for the spurt vacuum pump is rapidly increasing [1]. Together with minimizing the clogging of the spurt vacuum pump, the development of the impeller to optimize efficiency in a wide driving range of design techniques is required, due to the characteristics of the spurt vacuum pump with solids transfer. In particular, the configuration of the impeller is a crucial component that affects the spurt vacuum pump performance, because accurately understanding the flow pattern depending on its configuration may be the basis for optimal design. As computer technology has improved, CFD has recently become an alternative method to predict the internal flow field, which has thus been studied by many researchers using CFD codes. Kim et al. [2] conducted a study on the effect of variable inducer inlet angles on the hydraulic performance of the self-priming vacuum pump under a variety of rotational speeds and flow rate conditions. Patel et al. [3] concentrated on the effect of different impeller blade exit angles on the performance of the centrifugal pump. Gandhi et al. [4] experimentally investigated a centrifugal slurry pump to find applicability in accordance with the changes in the pump speed by using water and slurries at low solid concentrations (<20% by weight). Jin et al. [5] carried out numerical analysis on a centrifugal pump used in the industry to investigate the effect of the cross-sectional shape changes of the spiral casing on the performance curve. Choi et al. [6] studied the hydraulic performance excluding the cavitation phenomenon of the inducer, and indicated the inducer performance according to flow rate. Pagalthivarthi et al. [7] numerically investigated the effect of the casing configuration of the centrifugal pump, and provided physical insight into the flow field of the dense slurry in the centrifugal pump casing under different operational and geometric conditions. Yue et al. [8] carried out numerical analysis on the dry scroll pump to predict the transient flow under viscous flow by using CFD software. Gonzalez et al. [9] conducted a numerical analysis on the interaction between impeller and volute casing in the centrifugal pump by using a finite volume commercial code, and observed the secondary flow pattern in the centrifugal pump. Numerous studies of the impeller configuration in the centrifugal slurry pump have been investigated. However, few studies have addressed the effect of geometric impeller configurations on the performance of the spurt vacuum pump. In this study, the effects of the impeller discharge angle on the performance of the spurt vacuum pump were numerically considered. In particular, the performance of the spurt vacuum pump was evaluated on the basis of the correlations between the total head, pressure distribution, and pump efficiency.

*Corresponding author
E-mail: yjkim@skku.edu

II. Numerical Analysis

1. Rference model

Figure 1 shows a schematic of the spurt vacuum pump. The spurt vacuum pump that can transfer slurry and sewage by a specially designed impeller was selected as the reference model. The viscosity fluid containing solids and debris can be smoothly transferred through the flow passage without interference, since unlike other impellers, the impeller of the spurt vacuum pump is composed of one vane [10]. The casing diameter (D_1) is 370 mm, the impeller diameter (D_2) is 275 mm, the height of the pump casing (h_1) is 157 mm, the pump inlet diameter (D_3) is 100 mm, and the pump outlet diameter (D_4) is 220 mm. Three-dimensional (3D) geometry was designed using UG NX Ver. 8.5 and ANSYS Ver. 16.1 Design Modeler. Table 1 shows the discharge angle (β), which is the parameter of this study, and Fig. 2 describes the variable discharge angle of the impeller.

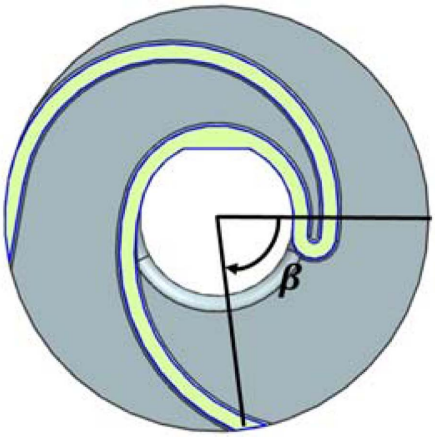

Figure 2. Design parameters of the Spurt vacuum pump.

2. Grid systems and boundary conditions

Grid systems were generated by applying tetrahedron grids to the pump casing, and hexahedron grids to the impeller region for more accurate simulation (refer to Fig. 3). In addition, the inflation grid condition was applied to the casing with 10 layers. In order to evaluate the grid dependency and determine the number of grid elements, the number of the elements in the grid system was changed from 100,000 to 1,000,000 for the total head. Figure 4 shows that the total head remained constant with over 500,000 elements. Thus, the number of grid elements of the spurt vacuum pump was set to 500,000 elements.

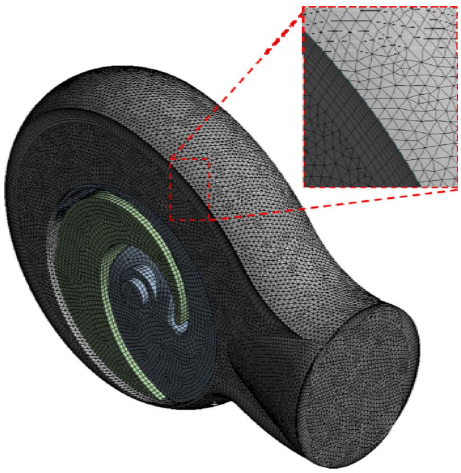

Figure 3. Grid systems.

Table 1 Parameter considered in this study

Cases	β [deg.]
Case 1	59.7
Case 2	64.7
Case 3	69.7
Case 4 (Ref.)	74.7
Case 5	79.7
Case 6	84.7
Case 7	89.7

The numerical calculation was conducted using the commercial code, ANSYS CFX 16.1. As for the boundary conditions, the working fluid was water with a mass flow rate of 58.16 kg/s (refer to Fig. 5). The effect of the rotating impeller was considered by applying the Moving Reference Frame (MRF) method, which separates the flow region into rotating and stationary regions. The Shear Stress Transport (SST) model was adopted, since it has shown to be a suitable turbulence model with fluid machine analysis when a steady-state analysis is performed [11]. The total pressure

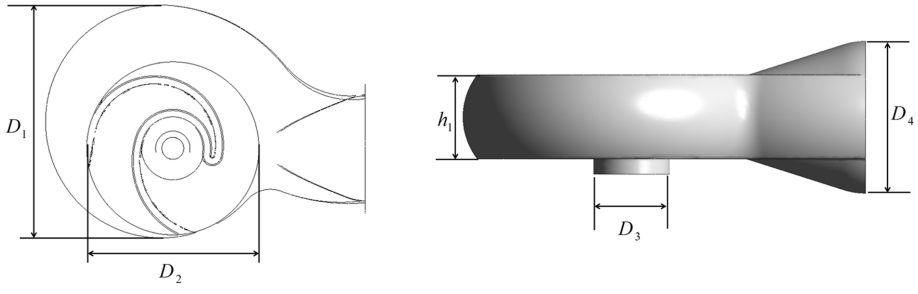

(a) Top view (b) Front view

Figure 1. Schematic of the Spurt vacuum pump.

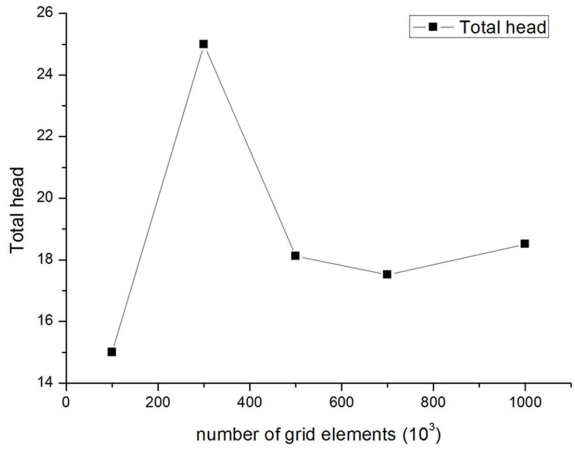

Figure 4 Grid dependency.

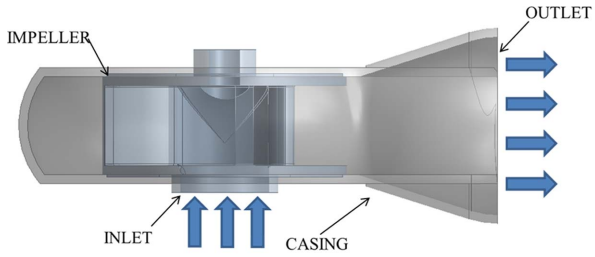

Figure 5 Boundary conditions.

Table 2. Flow and geometrical conditions applied in this study.

Rotating velocity [RPM]		1800
Working Fluid		Water
Turbulence model		Shear stress transport
Rotational domain		Moving reference frame
Inlet	Pressure [kPa]	0
Outlet	Mass flow rate [kg/s]	58.16
Interface condition		Frozen rotor
Convergence criteria		1e-4

condition was adopted to the inlet, with the mass flow rate condition applied to the outlet. The no-slip wall condition was applied to the pump casing. A frozen rotor condition, which can consider all the information of the grids, was employed at the entire interfaces. Table 2 gives the detailed boundary conditions.

3. Pump performance

The performance of the spurt vacuum pump can be evaluated by indicators such as efficiency and total head. In this study, the pump performance was evaluated using total head and pump efficiency. When the power given to the fluid by the pump is the water power and the power required to actually drive the pump is the shaft power, the ratio of the water power to the shaft power is called the efficiency of the pump. The pump efficiency (η) and total head (H) were calculated in the spurt vacuum pump, as follows:

$$\eta = \frac{\rho g H Q}{T\omega} \quad (1)$$

where is the water density (kg/m^3), is volumetric flow rate (m^3/s) and indicates the motor torque ($N \cdot m$).

$$H = \frac{P_o - P_i}{\rho g} \quad (2)$$

where in the inlet pressure (Pa), P_o denotes the outlet pressure (Pa).

III. Results and Discussion

1. Validation

In order to verify the reliability of the numerical results, Fig. 6 compares the results of the total head with the existing experimental data for the spurt vacuum pump [11]. The flow rate, size, and rotational velocity of model 22 are the same as those of the reference model. The total head of the reference model was 18.245 m. The numerical results of the total head were in good agreement with the experimental results.

2. Effect of angle variation

Figure 7 shows the results of the total head and pump efficiency under different discharge angles of 59.7°, 64.7°, 69.7°, 74.7°, 79.7°, 84.7°, and 89.7°, respectively. In all angular cases, the total head in cases 1, 2, 6 and 7 was higher than the reference model. In addition, the case 2 model showed a total head of 21.58 m, 17.3% higher than

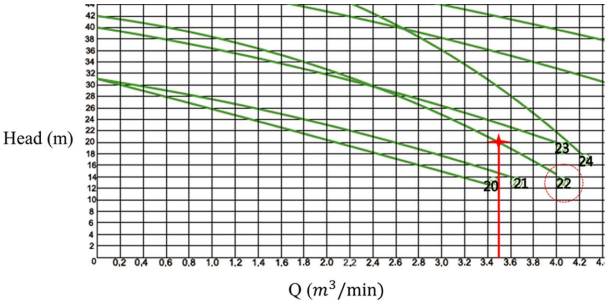

Figure 6. Comparison of the results of the total head between the present study and existing experimental data [11].

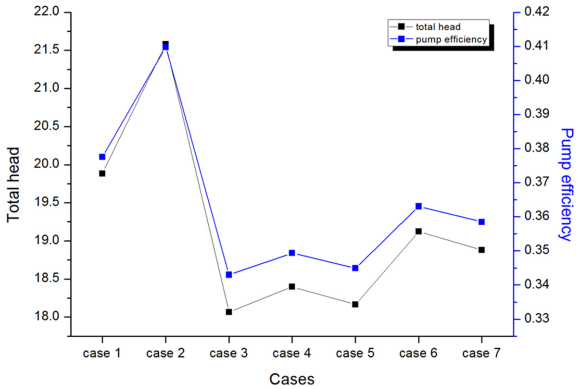

Figure 7. Pump efficiency and head for angle variations of discharge angle.

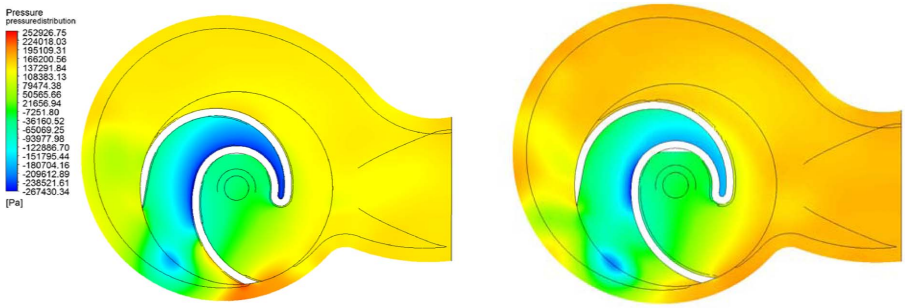

(a) Reference model (b) Case 2

Figure 8. Pressure distribution.

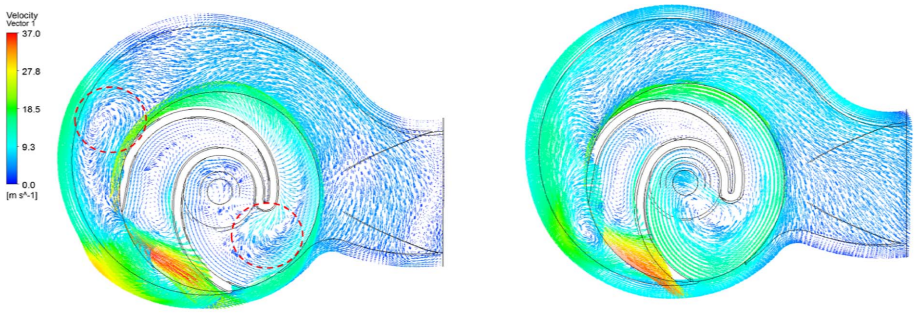

(a) Reference model (b) Case 2

Figure 9. Velocity vector distribution.

that of the reference model. When the discharge angle was varied back and forth under 5°, the pump performance was marginal; while when the discharge angle was changed from −5° to −10°, the pump performance was influenced.

3. Pressure distribution

Figure 8 shows the pressure distribution of the reference model and case 2 in top view. Note that a low-pressure region is formed in the vicinity of the inlet, and a high-pressure region is evident in the vicinity of the outlet. The working fluid obtains higher kinetic energy by the rotating impeller, since the decreased discharge angle increases the area of the discharge port, transferring the higher force. However, when the discharge angle has a smaller value than −10°, the efficiency is reduced,

since the frictional force caused by the increased area affects it. In addition, the pressure in the vicinity of the outlet in case 2 is higher than in the reference model. The results indicate that high pressure with high kinetic energy can discharge a greater amount of working fluid.

4. Velocity vector distribution

Figure 9 shows flow fields that are generated by the rotational rotor through the velocity vector fields. Water is pumped into the inlet of the pump, flows through the impeller of the pump, and quickly discharges from the outlet of the pump. By comparing the distribution of the velocity vector profiles, flowback around the impeller and a vortex field in the vicinity of the discharge port of the impeller were observed. However, Fig. 9(b) shows that in case 2, the variety in the vicinity of the impeller in which the moving of water was disturbed was decreased. It is considered that the vortex fields generated in the vicinity of the impeller can interrupt the circulation flow in the pump, and cause vortex fields in the casing. Thus, the configuration of the discharge angle of the impeller can be designed with alternative profiles, in order to obtain higher pump performance.

IV. Conclusions

In this study, the effects of the impeller discharge angle on the performance were numerically investigated for 7 cases. The total head and pump efficiency were greatest at the discharge angle of 64.7°. The pump performance was not influenced by the discharge angle when the angle was in the range of 5° back-and-forth. On the other hand, the pump performance was the greatest while the discharge angle changed from −5° to −10°. In addition, pump performance of relatively high pump efficiency and total head were derived with about a 17% increase in efficiency.

V. Nomenclature

β: Angle of discharge angle of impeller
η: Pump efficiency
ρ: Water density (kg/m^3)
Q: Volumetric flow rate (m^3/s)
T: Motor torque (Nm)
P_i: Inlet pressure (Pa)

P_o: Outlet pressure (Pa)

Acknowledgements

This research was supported by a grant (16IFIP-B089065-03) from the Plant R&D Program, funded by Ministry of Land, Infrastructure and Transport of the Korean Government.

References

[1] J. E. Yun, 2011, "CFD Analysis of Submersible Slurry Pump with Two Blades", Spring Conference of the Korean Society of the Mechanical Engineers, ISSN 1226-4881, pp. 263-268 (in Korean).
[2] J. W. Kim, H. S. Seo, H. G. Ji, Y. K. Jung, and Y. J. Kim, 2014, "Effect of Inducer Inlet Angles on the Performance of Self-priming Vacuum Pump", Autumn Conference of the Korean Society of Mechanical Engineers, pp. 126-131 (in Korean).
[3] M. G. Patel, and A. V. Doshi, 2013, "Effect of Impeller Blade Exit Angle on the Performance of Centrifugal Pump", International Jounal of Emerging Technology and Advanced Engineering, Vol. 3, Issue 1, pp. 702-706.
[4] B. K. Gandhi, and S. N. Singh, V. Seshadri, 2002, "Effect of Speed on the Performance Characteristics of a Centrifugal Slurry Pump", Journal of Hydraulic Engineering, Vol. 128, No. 2, pp. 225-233.
[5] H. B. Jin, M. J. Kim, C. H, Son, and W. J. Chung, 2012, "Spiral Casing of a Volute Centrifugal Pump-Effect of the Cross Sectional Shape- ", The KSFM Journal of Fluid Machinery, Vol. 16, No. 4, pp. 28-34 (in Korean)
[6] C. H. Choi, G. S. Lee, J. H. Kim, and S. S, Yang, 2001, "Numerical Study on the Hydrodynamic Performance Prediction of Turbopump Inducers", Spring Conference of the Korean Society of the Mechanical Engineers, pp. 625-630 (in Korean).
[7] Krishnan V. Pagalthivarthi, Pankaj K. Gupta, Vipin Tyagi, and M. R. Ravi, 2011, "CFD Predictions of Dense Slurry Flow in Centrifugal Pump Casings", World Academy of Science, Engineering and Technology International Journal of Mechanical, Aerospace, Industrial, Mechatronic and Manufacturing Engineering, Vol. 5, No. 3.
[8] Xiang-Ji Yue, Yan-Jun Lu, Ying-Li Zhang, De-Chun Ba, and Guang-Yu Wang, 2015, "Computational Fluid Dynamics Simulation Study of Gas Flow in Dry Scroll Vacuum Pump", Science Direct, Vol. 116, pp. 144-152
[9] Jose Gonzalez, Joaquin Fernandz, Eduardo Blanco, and Carlos Santolaria, 2002, "Numerical Simulation of the Dynamic Effects Due to Impeller-Volute Interaction in a Centrifugal Pump", Journal of Fluid Engineering, Vol. 124, pp. 348-355.
[10] H. H. Shin. (2011). "Impeller for Spurt Pump and Spurt Pump for Underwater Having Thereof", KR Patent 10-2010-0060743.
[11] Sinhan pump tech, Catalogue of high-efficiency Spurt Vacuum Pump, http://www.1181.co.kr/.